Algal Research 9 (2015) 170–177

Contents lists available at ScienceDirect

Algal Research

journal homepage: www.elsevier.com/locate/algal

Evaluation of wavelength selective photovoltaic panels on microalgae growth and photosynthetic efficiency

Angela M. Detweiler [a,b], Cécile E. Mioni [c], Katie L. Hellier [d], Jordan J. Allen [e], Sue A. Carter [d], Brad M. Bebout [a], Erich E. Fleming [f], Carley Corrado [d], Leslie E. Prufert-Bebout [a,*]

[a] NASA Ames Research Center, Exobiology Branch, Moffett Field, CA 94035, USA
[b] Bay Area Environmental Research Institute, Petaluma, CA 94952, USA
[c] California State University Monterey Bay, Science & Environmental Policy Division, Seaside, CA 93955, USA
[d] University of California Santa Cruz, Department of Physics, Santa Cruz, CA 95064, USA
[e] Colorado State University, Department of Atmospheric Science, Fort Collins, CO 80523, USA
[f] California State University Channel Islands, Department of Biology, Camarillo, CA 93012, USA

ARTICLE INFO

Article history:
Received 1 December 2014
Received in revised form 22 February 2015
Accepted 4 March 2015
Available online 25 March 2015

Keywords:
Microalgae cultivation
Growth rate
Wavelength selective luminescent solar concentrators
Photovoltaic cells
Greenhouse

ABSTRACT

Large-scale cultivation of microalgal biomass in open systems can benefit from the low cost of using natural sunlight, as opposed to artificial light, but may encounter problems with photoinhibition, high evaporation rates, potential contamination and high energy demand. Wavelength selective luminescent solar concentrator (LSC) panels can solve some of these problems when incorporated into low-cost sheltered structures for algal biomass production that concurrently produce their own electricity by harnessing select portions of solar energy, not used for algal growth. The LSC panels in this study contained a fluorescent dye, Lumogen Red 305, which transmits blue and red wavelengths used for photosynthesis with high efficiency, while absorbing the green wavelengths and re-emitting them as red wavelengths. The fluorescently generated red wavelengths are either transmitted to boost algal growth, or waveguided and captured by photovoltaic cells to be converted into electricity. We found that different strains of microalgae (currently used commercially) grew equally well under the altered spectral conditions created by the luminescent panels, compared to growth under the full solar spectrum. Thus this technology presents a new approach wherein algae can be grown under protected, controlled conditions, while the cost of operations is offset by the structure's internal electrical production, without any loss to algal growth rate or achievable biomass density.

Published by Elsevier B.V.

1. Introduction

The harvest of metabolic compounds from microalgae for the production of nutraceuticals, bioplastics, biofuels, cosmetics, animal feed, and other natural products has become of increasing interest in recent years, particularly as some of these replace petroleum based products [1–3]. Although technological and biological optimization of microalgal biomass production is constantly evolving, growing large quantities of algae in open and closed cultivation systems in an economically viable and sustainable manner is still a challenge. The electrical requirement through all steps from cultivation, harvesting, and product extraction is a major sink of resources [4,5]. One way to supplement energy needs is the production of electricity within the plant *via* anaerobic digestion of less valuable biomass [6]. A more direct approach is the use of luminescent solar concentrator (LSC) panels, which can absorb solar radiation and convert light of specific wavelengths into electricity *via* photovoltaic cells [7].

Luminescent solar concentrators were first developed in the 1970s, but have gained renewed interest in recent years with the improved stability and resistance of organic dyes [7–10]. A transparent panel is infused or coated with luminescent organic dyes or quantum dots (semiconductor nanocrystals). Light is collected by fluorescent particles distributed over a large surface area and is re-emitted as longer wavelengths, which are then guided within the panel by total internal reflection and are concentrated onto solar cells, usually located on the edge of the panels [7,8].

The LSC panels used in this study, described in Corrado et al. [10], were infused or coated with a fluorescent organic dye, Lumogen Red 305 (LR305), which absorbs wavelengths shorter than 400 nm and green wavelengths between 500–600 nm, re-emitting the latter as longer wavelengths in the 600–750 nm range. About 80% of the red light is trapped and waveguided in the panels, a significant portion of which is captured by front-facing photovoltaic (PV) cells and converted to electricity, while half of the remaining 20% of light causes enhanced red light illumination beneath the panels (see Fig. 1 in Corrado et al. [10]).

* Corresponding author at: NASA Ames Research Center, Mail Stop 239-4, Bldg. 239, Room 334, P.O. Box 1, Moffett Field, CA 94035, USA.
E-mail address: leslie.e.bebout@nasa.gov (L.E. Prufert-Bebout).

http://dx.doi.org/10.1016/j.algal.2015.03.003
2211-9264/Published by Elsevier B.V.

The transmission of the LSC panels is dependent on the concentration of the dye used.

LSC panels can easily be installed on existing greenhouse structures to provide an enclosed space with reduced evaporation rates, and reduced photoinhibition due to the selective spectrum, while also producing energy for greenhouse operations using the green photons which are of lower value to photosynthetic organisms [11]. Currently, these panels can produce ~50 W/m^2 on a sunny day (they will also produce energy on a cloudy day by efficiently capturing diffuse light) and, dependent on the scale of production, can cost as little as $100/m^2 one-time cost for panels with a twenty-year or more lifetime (personal communication C. Corrado).

The maximum transmission of the LR305 panels in the blue and red wavelength bands correlates well with the maximum absorbance of photosynthetic pigments. The absorbed green light, which is re-emitted as longer wavelengths, provides an additional source of red light, making these panels ideal for cultivating microalgae, cyanobacteria and plants. Photosynthetic organisms are generally green because they reflect light with wavelengths in the green region of the visible solar spectrum. Algae have photosynthetic pigments (chlorophyll *a*, *b*, *c*, and *d*) that absorb light in the blue (~420–480 nm) and red (~620–680 nm) regions of the photosynthetic active radiation (PAR) spectral range (400–700 nm) [12]. Other accessory photosynthetic and photoprotective pigments, such as carotenoids absorb light between 420–500 nm. Aside from chlorophyll *a* (chl *a*), cyanobacteria also have light-harvesting antennae called phycobilisomes containing pigments (*e.g.*, phycocyanin and phycoerythrin) that absorb green, yellow and orange light (~490–650 nm) [12,13].

Any technology that results in changes to the light field experienced by photosynthetic organisms (such as greenhouse panels), particularly ones being raised for commercial products, needs to take into account the effect of the spectrum of available light on growth and product formation rates. The importance of light quality for algae growth and cell composition has been investigated using light-emitting diodes (LEDs) in short-term experiments and at low irradiance levels in laboratory settings. Studies by Lee and Palsson [14], Matthijs et al. [15], and Gordon and Polle [16] suggested that monochromatic red light enhances algal growth rates compared to white light. Fu et al. [17] found that *Dunaliella salina* had higher biomass production and carotenoid (β-carotene and lutein) accumulation at a higher irradiance (170 μE m^{-2} s^{-1}) when 75% red and 25% blue light were combined, compared to red light alone. Katsuda et al. [18] observed that *Haematococcus pluvialis* showed increased concentrations of astaxanthin, at a cost of cell growth suppression under purple-blue light (380–470 nm), compared to red, green, blue, purple and fluorescent light at extremely low light intensities (2–12 μE m^{-2} s^{-1}). Das et al. [19] grew *Nannochloropsis* sp. over a period of 8 days, under white, green, red and blue light, and found that growth rates were higher under blue light alone.

Overall, these light quality studies and many others demonstrate that at least red and/or blue light are essential for the growth of algae. These observations were the impetus to study the growth of algae using solar radiation filtered through LSC panels that transmit blue and red wavelength bands, while retaining most of the green wavelengths for electricity production. Thus, the objective of this study was to compare growth rates, photosynthetic efficiency and pigment production in various green algae and cyanobacteria grown under spectrally selective LSC panels containing the dye LR305 and a clear, standard type greenhouse.

2. Materials and methods

2.1. Algae strains

Four strains of microalgae (*Chlorella vulgaris*, *D. salina*, *Chlamydomonas reinhardtii*, *Botryococcus sudeticus)* and a cyanobacterium (*Spirulina platensis*) (see Table 1 for strain information), were chosen for this study due to commercial interest in their pigments, proteins, lipids and/or other nutritional values [1,2,20]. The cultures were grown in media shown in Table 1 using aseptic techniques to minimize contamination.

2.2. Growth experiments

2.2.1. Small batch cultures of algae grown under LSC panels with different LR305 dye concentrations

Algae cultures were started indoors in 2 L Erlenmeyer flasks placed on a gyratory shaker (New Brunswick Scientific — model G10, New Brunswick, NJ) under "cool-white" light (Phillips — model F32T8/TL741, Alto, Somerset, NJ — color temperature 4100 K). Cultures were then gradually adapted to ambient near full solar light in a greenhouse, using increment reduction in neutral density screening, over a period of 2–3 days prior to performing growth experiments at NASA Ames Research Center (ARC), Moffett Field, CA (37°25′38″N, 122°3′43″W).

The acclimated cultures were transferred into fresh media (see Table 1 for respective medium for each strain) to a final optical density at 750 nm (OD_{750}) of 0.1. One hundred mL aliquots of the diluted culture were transferred to twelve 250 mL Erlenmeyer flasks. Triplicate flasks were placed in four different acrylic aquaria filled with water for temperature control. Submersed aluminum tubes with circulating water from an aquarium chiller (AquaEuroUSA — model MC ½ HP, Gardena, CA) reduced water temperature fluctuations in the aquaria. Water temperature in each aquarium was measured every 10 min using temperature loggers (Onset Hobo Water Temp Pro v2 — model U22-001, Bourne, MA). Water temperature varied between 15.8 °C and 23.8 °C, with an average of 18.5 °C.

Irradiance was measured as PAR using a LI-COR quantum sensor (model LI-190SA) coupled with a LI-1400 data logger (LI-COR, Lincoln, NE). The NASA ARC greenhouse was covered with Acrylite OP-4 sheets (Cyro Industries, Parsippany, NJ) which allows for 80% light transmission around 300 nm, and ~92% transmission >400 nm of the solar UV to pass through. Irradiance measurements inside the greenhouse, adjacent to the LSC panels, reached 1090 μE m^{-2} s^{-1} in the winter, with an average day/night irradiance of 201 μE m^{-2} s^{-1}. During the summer, irradiance measurements reached 1529 μE m^{-2} s^{-1}, with an average day/night irradiance of 382 μE m^{-2} s^{-1}.

Flasks were topped with rubber stoppers and bubbled with air filtered through a 0.2 μm syringe filter (Fisher Scientific part #194-2520, Waltham, MA) to provide adequate airflow in the flasks and to maintain the algae in suspension. Three of the aquaria containing flasks of algae were covered with LSC panels containing different concentrations of the dye LR305; these were designated LSC light, LSC medium and LSC dark hereafter. The fourth aquarium was covered with a clear acrylic panel and served as the control (Fig. 1A).

2.2.2. Spectra transmitted through LSC and clear panels

The spectral composition of light transmitted through the LSC panels and the clear panel was measured (between 350–800 nm) with a spectrometer (Ocean Optics — model USB4000-VIS-NIR, Dunedin, FL) and normalized to the solar spectrum (Fig. 2). There was decreasing transmittance of purple and blue (~400–495 nm) and green (~495–570 nm) light with increasing dye concentration. The amount of transmitted red light with wavelengths between 600 and 730 nm was similar for all three dye concentrations, and exceeded the red light transmittance of the control panels above 630 nm. The transmittance (PAR) of the clear panel, and LSC light, medium and dark panels at peak irradiance were 98%, 77%, 66% and 60%, respectively, in relation to full solar irradiance.

2.2.3. Fifty-liter raceway cultures of D. salina grown in an LSC and a clear greenhouse

To investigate the effect of LSC light filtration on the growth rates of large scale cultures, the green alga *D. salina* was grown in 50 L raceways in a greenhouse with LSC medium panels as well as in a separate greenhouse with clear panels (also referred to as control) (Fig. 1B) at the

Table 1
Organism, strain type and culture media used in experiments.

Class	Organism	Strain	Media
Chlorophyceae	*Chlamydomonas reinhardtii*	CC 1690	P49
	Botryococcus sudeticus	UTEX 2629	ATCC BG11 +
Cyanophyceae	*Spirulina platensis*	ATCC 29408	*Spirulina* medium [21]
Trebouxiophyceae	*Chlorella vulgaris*	ATCC 30581	ATCC 847
	Dunaliella salina	CCAP 19/18	ATCC 1174 DA or Instant Ocean Aquarium Sea Salt Mixture (mod.)

University of California Santa Cruz (UCSC), Santa Cruz, CA (36°59′29″N, 122°3′39″W). First, two 2 L stock cultures were prepared and acclimated to ambient solar light using the methods described in Section 2.2.1. The medium used for the stock culture as well as the raceways consisted of an artificial seawater medium (Instant Ocean — Aquarium Sea Salt Mixture, Blacksburg, VA) — 35 g/L, with the addition of 1 mL/L of the following stock solutions: 36.3 mM KH_2PO_4 F/2, A5 trace metal (g/L: 2.86 H_3BO_3; 1.81 $MnCl_2$*$4H_2O$; 0.222 $ZnSO_4$*$7H_2O$; 0.39 $NaMoO_4$*$2H_2O$; 49.4 mg $Co(NO_3)_2$*$6H_2O$), 11.7 mM Fe-EDTA, 0.88 M $NaNO_3$, and vitamin mix F/2 (mg/L: 0.5 Cyanocobalamin vitamin B12; 0.5 Biotin; 200 Thiamin vitamin B1); salinity 35 ppt, pH 8. Raceways were inoculated with 700 mL of stock culture with an OD_{750} of 0.6. Raceways were continuously mixed using paddle wheels, resulting in a flow rate ranging from 0.1–0.2 m/s in the raceways. For each light condition, raceways were operated in triplicate.

Vernier sensors coupled to a LabQuest 2 interface (Beaverton, OR) were used to measure water temperature (#TMP-BTA), pH (#PH-BTA), salinity (#SAL-BTA), electrical conductivity (#CON-BTA) and flow rate (#FLO-BTA) at intervals of 2–3 days for an 18-day growth period. Nutrient samples were filtered using a 0.45-μm sterile cartridge filter and kept frozen (−80 °C) until processing on a Lachat flow-injection analyzer at the Institute of Marine Sciences Marine Analytical Lab at UCSC. Ammonium N (NH_4^+-N) was analyzed using the salicylate method, nitrate + nitrite N (NO_x-N) was analyzed using the cadmium reduction method, and orthophosphate (PO_4^{3-}) was analyzed using the ascorbic acid method. The calibration standards and quality controls were prepared using the following Hach standard stock solutions (Hach Company, Loveland, CO): nitrate (#307-49), phosphate (#14204-16) and ammonium (#153-49). Each sample run included a certified reference material (Wastewater effluent certified reference material: Hach # 28332-49). Variations in salinity due to evaporation were corrected if necessary by adding tap water at each sampling date. Air and water temperature in the greenhouses were not controlled. Average raceway water temperature in the clear and the LSC greenhouses ranged from 15.8 to 23.5 °C and 15 to 23.5 °C, respectively, with a maximum difference of 2.2 °C between greenhouses on day 4 of the experiment.

Photosynthetically active radiation was measured at 10 min intervals in each greenhouse at UCSC using Apogee quantum sensors (model SQ-110, Logan, UT) coupled with CR1000 Campbell Scientific data loggers (Logan, UT). During the 18-day experiment at UCSC, irradiance in the clear greenhouse varied from 0–1734 μE m^{-2} s^{-1}, with an average day and night time reading of 398.5 ± 566.2 μE m^{-2} s^{-1}. A linear regression of the irradiance in the clear *vs.* the LSC greenhouse indicated that irradiance in the LSC greenhouse was equivalent to 45% (±0.7% SE) of the irradiance seen in the clear greenhouse.

2.3. Measurement of cell density and growth rate

For the small batch culture experiments performed at NASA ARC, optical density (OD_{750}) was measured every day over a period of 4–5 days using a Shimadzu UV-1800 spectrophotometer (Shimadzu, Kyoto, Japan). For the raceway culture experiments performed at UCSC, a Hach DR2700 portable spectrophotometer (Hach, Loveland, CO) was used to measure OD_{750} every 2–3 days. Algal cell density or cell dry weight was calculated using optical density measurements and previously established calibration curves for each strain.

Cell enumeration was performed for *C. vulgaris*, *C. reinhardtii* and *D. salina* using a Neubauer chamber and a Nikon Microphot-FXA microscope (Nikon, Melville, NY). Cell dry weight was measured for *S. platensis* and *B. sudeticus*. After measuring the OD, a known volume of culture was filtered through pre-weighed GF/F filters (25 mm dia.) (GE Healthcare Bio-Sciences, Pittsburgh, PA) and placed in an oven at 80 °C for 24–48 h. Filters were then weighed again and the biomass was calculated in mg/mL (adapted from Steinman and Lamberti [22]). Filters were weighed using an analytical balance with a 0.1 mg precision (Mettler Toledo — model MS204S, Columbus, OH).

Growth rate (μ) was determined individually for each replicate using a linear regression of the log transformed cell density over time according to Eq. (1):

$$\mu = \ln(N_t - N_0)/(t - t_0) = \text{slope}. \quad (1)$$

Doubling time (t_d) was calculated using the following equation:

$$t_d = (\ln 2)/\mu. \quad (2)$$

Only data collected during the exponential growth phase were used for growth kinetic analyses.

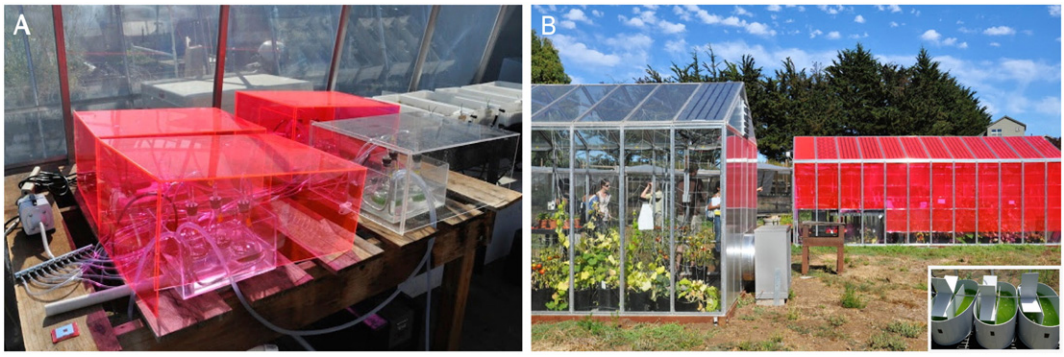

Fig. 1. Experimental set-up at NASA ARC — triplicate flasks of algae cultures were placed in water baths underneath three different LSC panels containing different concentrations of the LR305 dye and a clear panel (A). Experimental set-up at UCSC — *D. salina* cultures were grown in triplicate raceways (culture volume 50 L) under a clear (left) and an LSC medium (right) covered greenhouse (B). Figure available in color online.

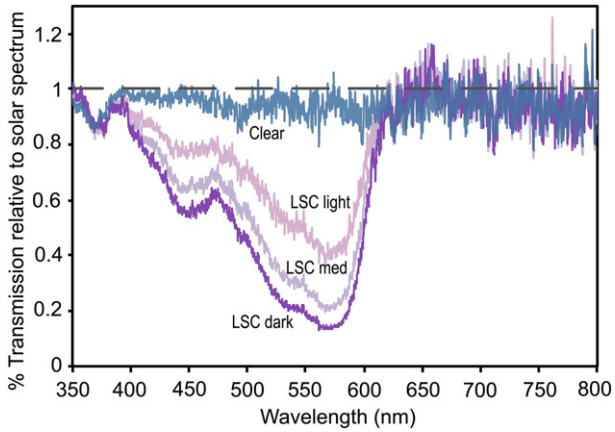

Fig. 2. Transmission spectra (350–800 nm) for the three LSC panels and the control panel relative to the solar spectrum recorded outside on a clear day. All spectra were normalized to the solar spectrum, which is represented by a dashed line. Figure available in color online.

2.4. In vitro absorption spectra

The absorption maxima for photosynthetic and photoprotective pigments within the 400–700 nm spectral band were measured spectrophotometrically for the different cultures to assess any pigment shifts related to the spectral transmission of the LSC panels.

For the small batch cultures, pigment extractions were performed on culture samples at the end of the 4–5 day experimental run. A known volume of culture was filtered through a Whatman GF/F glass fiber filter (25 mm) and placed in a glass scintillation vial containing a known volume of 100% methanol (MeOH), buffered with magnesium carbonate ($MgCO_3$) to minimize conversion of chl *a* to pheophytin. Vials were kept in the dark at 4 °C for 24 h. Then, samples were transferred to 2 mL Eppendorf tubes and centrifuged for 5 min at 15,000 rpm to precipitate out any particles from the supernatant. The solvent containing the extracted pigments was analyzed on the Shimadzu spectrophotometer, using a 1 cm width quartz cuvette. Chl *a*, total carotenoids (car), and chl *b* (if present) were quantified using the equations in Lichtenthaler and Buschmann [23].

For the 50 L raceways, *D. salina* culture samples were collected for measurement of chl *a* concentration from each replicate raceway at the beginning of the experiment (day 0), during the exponential growth phase (day 7) and during the stationary phase (day 14, day 16). Samples (10–50 mL) were collected on GF/F filters and kept frozen (−80 °C) in the dark until analysis. Samples were extracted for 24 h in the dark at −20 °C in 90% acetone. Chl *a* concentrations were determined using a Turner fluorometer following the non-acidification method [24], using the following equation:

$$\text{Chl } a\ (\mu g/L) = (F_s - F_b) * 0.00025 * (V_e/V_f) * D; \quad (3)$$

where 0.00025 is the calibration constant in μg Chl/mL/RFU (relative fluorescence units); F_s and F_b are the fluorescence measurements for the sample and a blank (90% acetone), respectively; V_e and V_f are the extracted and filtered volumes, respectively; and D is the dilution ratio.

2.5. In vivo fluorescence intensity spectra

An excitation spectrum for chl *a* was generated for each culture at the end of the 4–5 day experiment. Emission intensity was measured at 680 nm (chl *a* emission maximum) while varying the excitation wavelength from 400–650 nm (at 5 nm intervals) using a Spectramax M5 microplate reader (Molecular Devices, LLC, Sunnyvale, CA).

2.6. Photosynthesis–Irradiance (PI) curves

A programmable 16-LED array (TeleLumen LLC, Saratoga, CA) was used to simulate the spectra of solar light as well as solar light transmitted through an LSC medium panel. The photosynthetic rate of *D. salina* was measured as a function of irradiance for each spectrum.

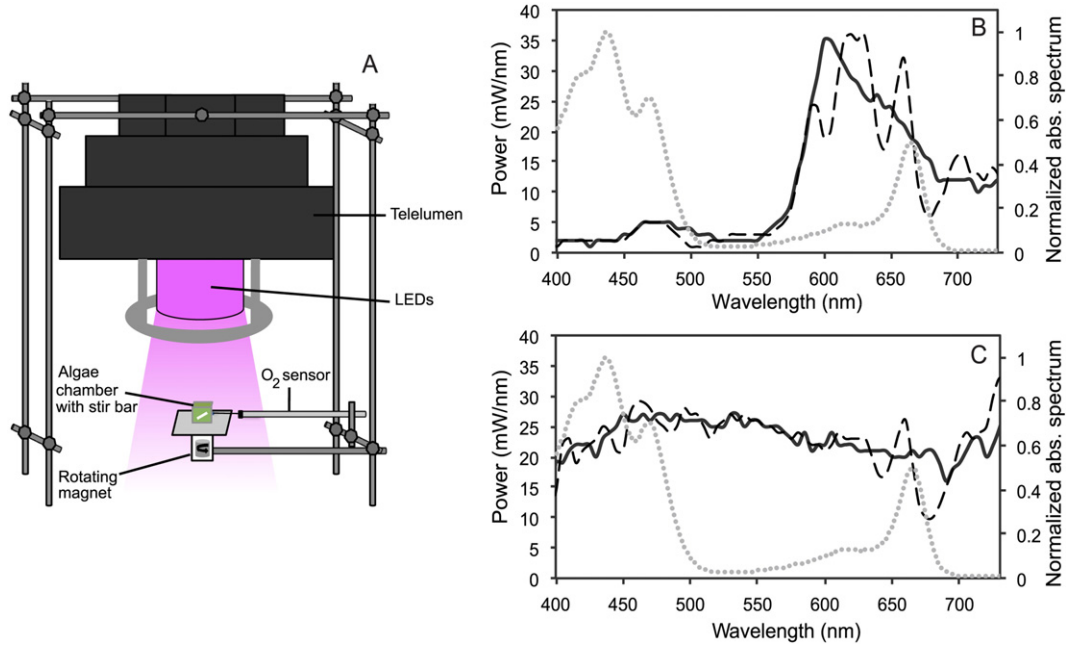

Fig. 3. Experimental schematic of LED light replicator and oxygen probe used to measure photosynthetic rates of algae under various spectral conditions (A). LSC medium (B) and the solar (C) spectra were recorded with a USB4000 spectrometer and simulated using the Telelumen Developer suite software. Relative spectral energy output by the Telelumen is presented on the left y-axis as mW/nm. On the right y-axis the absorption spectrum for pigments found in *D. salina in vitro* is represented by a dotted line, a solid black line represents the recorded spectrum, and a dashed line represents the simulated spectrum. Each spectrum was normalized to its own maximum absorption peak. Figure available in color online.

2.6.1. Culture preparation

D. salina was transferred to fresh media in 250 mL Erlenmeyer flasks and was placed on a gyratory shaker under "cool-white" light for 1–5 days prior to performing experiments. Irradiance on the surface of the shaker was ~50 μE m^{-2} s^{-1}.

2.6.2. Experimental setup

The solar spectrum and the spectrum transmitted through an LSC medium panel were recorded outside on a clear day using an Ocean Optics spectrometer. The recorded spectra were simulated with the light replicator controlled by the Telelumen Developer suite software within a 390–730 nm wavelength band range. Differences between the simulated spectrum and the captured spectrum were due to limitations in the LED array, particularly in the red region (590, 615, 630, 660 and 700 nm) (Fig. 3).

The *D. salina* culture was diluted to an OD_{750} of 0.1 and injected by syringe (~6 ml) into a $2 \times 2 \times 1.5$ cm^3 acrylic chamber containing a septum. A needle probe oxygen (O_2) sensor (PyroScience – Optical O_2 sensor – model OXR50, Aachen, Germany) was inserted through the septum to measure dissolved O_2 concentration (Fig. 3). Irradiance varied between 0–1000 μE m^{-2} s^{-1} and the O_2 concentration (μmol O_2 L^{-1}) 1) was recorded continuously for 5 min at each irradiance. The slope of the linear regression of O_2 concentration for each 5-minute segment corresponded to the O_2 production rate (μmol O_2 L^{-1} h^{-1}). Solar and LSC medium PI curves were run three to four times at each irradiance, using fresh cultures each time.

Oxygen production rates and irradiance values were plotted with the program OriginLab, V. 7.5 (Northhampton, MA) and fitted to a model in Platt et al. [26]:

$$P = P_s[1 - \exp(-\alpha I/P_s)][\exp(-\beta I/P_s)]; \quad (4)$$

where P_s is the scaling potential maximum photosynthetic capacity, α is the positive slope of the curve prior to photoinhibition, and β is the negative slope response due to photoinhibition.

Upon differentiation of Eq. (4), the maximum photosynthetic rate, P_{max}, can be written as [27]:

$$P_{max} = P_s[\alpha/(\alpha+\beta)][\beta/(\alpha+\beta)]\hat{}\beta/\alpha. \quad (5)$$

The standard error in P_{max} was calculated by propagating the standard errors in α, β and P_s that resulted from curve fitting.

2.7. Statistics

Statistical tests were carried out using GraphPad Prism v.6 (GraphPad Software, La Jolla, CA) and Microsoft Excel (Microsoft, Redman, WA). F-tests were performed to check for equal or unequal variance within treatments, followed by student t-tests to check for differences in growth rates, chl *a*, and carotenoid/chl *a* between the LSC and control treatments. For all analyses, a 95% confidence interval was used. Results were considered significant at $p < 0.05$ unless otherwise stated. Data were represented as the average ± standard deviation for triplicate cultures, unless otherwise stated.

3. Results and discussion

3.1. Growth rates

3.1.1. Small batch cultures

Fig. 4 shows the growth rates for the four different microalgae and a cyanobacterium under different LSC panels. *C. vulgaris* growth rate (Fig. 4b) was significantly higher and doubling time significantly lower under the LSC dark panel ($\mu = 0.29 \pm 0.03$ d^{-1}; $t_d = 2.44$ d) compared to growth under the control panel ($\mu = 0.23 \pm 0.01$ d^{-1}; $t_d = 2.98$ d) (t-test, $p_\mu = 0.026$; $p_{td} = 0.015$). The four other strains showed no statistical difference in growth rate or doubling time between the control and LSC treatments.

3.1.2. Raceway cultures

In the raceways, *D. salina* cultures grew exponentially from the inoculation date to day 7 in both the clear greenhouse and the LSC greenhouse (Fig. 5A), with no lag phase observed. Growth rates started declining after day 7 in both treatments and the cultures entered stationary phase around day 11. The observed decline of growth in both greenhouses was likely due to the depletion of nitrate and not

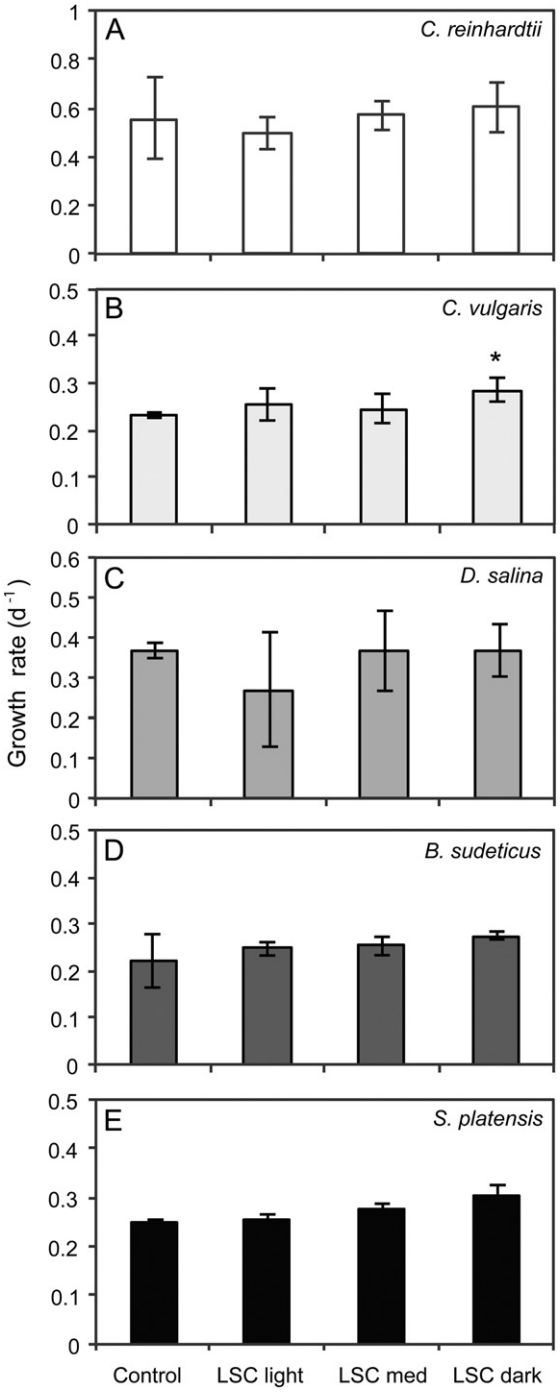

Fig. 4. Growth rates (μ) are represented by bar graphs for *C. reinhardtii* (A), *C. vulgaris* (B), *D. salina* (C), *B. sudeticus* (D) and *S. platensis* (E) with a starting optical density of 0.1 (OD_{750}). The asterisk indicates statistical difference (t-test, $p < 0.05$) between an LSC treatment and the control. Error bars represent standard deviation to the mean (N = 3) when larger than the symbol size.

phosphate. On day 11, the nitrate concentration was 0.02 ± 0.02 mg/L for the clear greenhouse cultures and below the detection limit for the LSC greenhouse cultures compared to an initial concentration of 2.75 ± 0.0 mg/L for both treatments on day 0. Phosphate concentrations declined from 3.74 ± 0.41 to 0.15 ± 0 mg/L for the clear greenhouse, and from 4.04 ± 0.21 to 0.19 ± 0.03 mg/L for the LSC greenhouse cultures in the same time duration.

There was no significant difference in growth rates (control: 0.34 ± 0.03 d^{-1}; LSC: 0.35 ± 0.01 d^{-1}) or doubling time (control: 2.05 ± 0.2 d; and LSC: 1.97 ± 0.07 d) (t-test, $p > 0.05$) between treatments (Fig. 5A). The total yield was also comparable in both treatments, plateauing around 3.27 × 10^6 cells/mL after 11 days.

3.2. Pigments

Chl *a* and carotenoid concentrations were reported in μg/10^6 cells for *C. vulgaris*, *C. reinhardtii* and *D. salina*, and in μg/mg of dry weight for *B. sudeticus* and *S. platensis* to account for the varied culture densities at the end of each experiment (Table 2).

Chl *a* content was slightly higher on average for *C. vulgaris* grown under all three LSC panels (0.15–0.16 μg/10^6 cells) compared to the control (0.12 μg/10^6 cells) (t-test, $p < 0.028$) (Table 2), and for *B. sudeticus* grown under the LSC light and dark panels (10.15–10.18 μg/mg dry weight) compared to the control (7.84 μg/mg dry weight) (t-test, $p < 0.023$). None of the other small batch cultures presented significant differences in chl *a* content between the LSC and the control treatments.

Total carotenoid concentrations were normalized to chl *a* concentrations. Carotenoid to chl *a* ratios varied between treatments for the different strains, but were only significantly lower under the LSC dark treatment compared to the control for *C. vulgaris* (t-test, $p < 0.0415$) and significantly higher under the LSC dark treatment compared to the control for *S. platensis* (t-test, $p < 0.0294$) (Table 2). Carotenoids absorb light in the near UV (360–400 nm) as well as between 400–550 nm [28–30] and can either harvest light for the photosynthetic reaction centers or act as photoprotective pigments, drawing energy away from the reaction centers. UV light transmission (<400 nm) was the same in the clear acrylic control and LSC panels. Transmission increased with decreasing dye concentration at wavelengths between 400–500 nm in the following order: LSC dark < LSC medium < LSC light < control (Fig. 2). The lack of a clear correlation between dye concentration and carotenoid production may be due to competition between carotenoids' dual roles as photoprotective and photosynthetic pigments, or alternatively may be due to the absence of UV trigger in all light treatments. In commercial applications, where carotenoids are the target product, the use of LR305 dye in LSC panels may not be beneficial, but other dye combinations with transmittance tailored to stimulate carotenoid production may be investigated.

In the *D. salina* raceway cultures, cellular chl *a* content was significantly higher in the LSC treatment relative to the control treatment during the late exponential phase (day 7) and early stationary phase (day 14) (paired two-tailed t-tests, $p < 0.05$, Fig. 5B). The higher cellular chl *a* content under the LSC panel is likely due to the lesser availability of photons with wavelengths corresponding to the absorption peaks of chl *a*. While the availability of photons at 680 nm was approximately equal for both greenhouses, the availability of photons at 435 nm was approximately 30% lower in the LSC greenhouse. Studies have shown that photosynthetic organisms growing in low light have increased pigmentation (larger chlorophyll antennae) to maintain the rate of energy delivery to the photosynthetic reaction centers [31]. The decrease in chl *a* in both treatments during the stationary phase (day 14 and 16) is likely attributed to N-limitation in both treatments. When algae are deprived of nitrogen, fewer amino acids are available and chlorophyll protein synthesis is reduced leading to a reduction in cellular chlorophyll content [32,33].

3.3. Fluorescence in vivo

There were no observable shifts in fluorescence emission spectra for the small batch algae cultures under the control *versus* the LSC treatments (data not shown). Fluorescence intensity profiles of emission at 680 nm for the green algae *C. reinhardtii*, *C. vulgaris*, *D. salina* and *B. sudeticus* showed bimodal peaks: one at 440 nm, which is within the range of absorption for chl *a* (420–440 nm); and a second peak at 475 nm, which is within the range for chl *b* and carotenoids (460–490 nm) [12,34]. The cyanobacterium *S. platensis* lacked excitation peaks for chl *a* and carotenoids (400 to 500 nm) while possessing a broad peak between 550–650 nm, which corresponds to the excitation peaks for phycobiliproteins (phycoerythrin and phycocyanin) [34]. Excitation maxima for chl *a* are the result of accessory pigments transferring radiant energy to chl *a* in the PSII reaction center [13,25]. Carotenoids, for example, mostly serve as a photoprotective UV pigment, but they can also act as an accessory pigment in photosynthesis [25,30].

The indication that, as expected for both control and LSC growth conditions, the blue region contributes to PSII reaction center in green algae suggests that blue light should not be completely removed for optimal biomass production. Whereas for cyanobacteria a large and significant portion of the blue light could be re-allocated to PV cells, since it does not appear to be as efficiently utilized. Our growth data further supports the hypothesis that some of the blue light can be re-allocated to PV without impacting growth rates in these organisms on a species to species basis, taking local, regional solar flux conditions into account.

3.4. LED array experiments

Photosynthetic efficiency of *D. salina* was measured as the rate of increase of O_2 production rate as a function of irradiance under simulated solar and LSC medium spectra, prior to the onset of

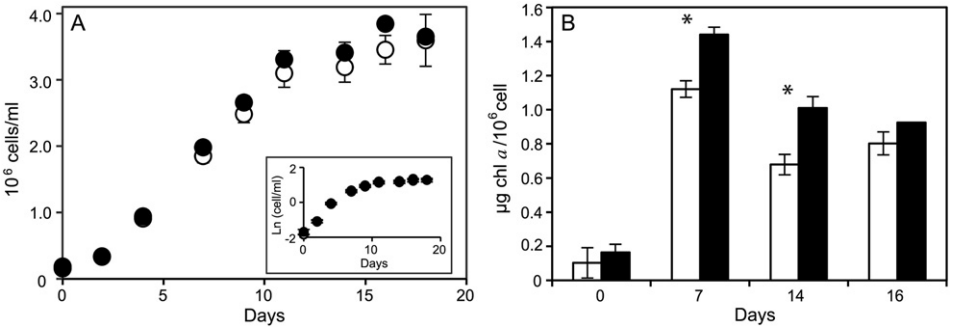

Fig. 5. Growth of *D. salina* in control (white circles) and LSC treatments (black circles), with the log transformed *D. salina* cell density over time as an inset (A). Only data points up to day 7 were considered for growth kinetic data analyses, representing the exponential growth phase. Cellular chl *a* content (μg chl *a*/cell) over time in the control (white bars) and LSC treatment (black bars) for *D. salina* raceway cultures (B). Asterisks indicate statistical difference (t-test, $p < 0.05$) between the LSC treatment and the control. Error bars represent standard deviation to the mean (N = 3).

Table 2
Chl *a* and car/chl *a* ratios determined spectrophotometrically from 100% methanol extracts of four microalgae and a cyanobacterium after four days growing under different shades of LSC panels. Chl *a* concentration for *C. vulgaris*, *C. reinhardtii*, and *D. salina* was measured in μg/10^6 cells, and for *B. sudeticus* and *S. platensis*, chl *a* was measured in μg/mg of dry weight. Chl *a* concentrations are represented as the average ± standard deviation for triplicate samples, unless noted otherwise.

	Chl *a* (μg/10^6 cells)				Car/chl *a*			
Organism	Control	LSC light	LSC med	LSC dark	Control	LSC light	LSC med	LSC dark
C. vulgaris	0.12 ± 0.01	0.15 ± 0.01[a]	0.16 ± 0.02[a]	0.16 ± 0.01[a]	0.68 ± 0.05	0.59 ± 0.01	0.59 ± 0.04	0.58 ± 0.02[a]
C. reinhardtii	2.29 ± 0.72	2.07 ± 0.48	1.31 ± 0.56	2.15 ± 0.07	0.44 ± 0.02	0.45 ± 0.01[b]	0.46 ± 0.01	0.40 ± 0.00
D. salina	1.44 ± 0.08	1.33 ± 0.25	1.08 ± 0.25	1.32 ± 0.14	0.53 ± 0.01	0.55 ± 0.02	0.53 ± 0.03	0.52 ± 0.02
	Chl *a* (μg/mg of dry weight)				Car/chl *a*			
Organism	Control	LSC light	LSC med	LSC dark	Control	LSC light	LSC med	LSC dark
B. sudeticus	7.84 ± 0.47	10.15 ± 0.32[a]	9.30 ± 1.98	10.18 ± 1.02[a]	0.54 ± 0.02	0.52 ± 0.02	0.52 ± 0.01	0.49 ± 0.02
S. platensis	3.78 ± 0.56	3.85 ± 0.28	3.97 ± 0.27	4.35 ± 0.5	0.59 ± 0.05	0.61 ± 0.01	0.63 ± 0.03	0.68 ± 0.02[a]

[a] LSC treatment statistically different from control (t-test, $p < 0.05$).
[b] Results based on duplicates.

photoinhibition (α). Photosynthetic efficiency was higher for the solar spectrum treatment (α = 2.49 ± 0.25 μmol O_2 L^{-1} h^{-1}/(μE m^{-2} s^{-1}), compared to the LSC medium treatment (α = 1.8 ± 0.26 μmol O_2 L^{-1} h^{-1}/(μE m^{-2} s^{-1}), which may be attributed to the spectral quality of the solar spectrum (Fig. 6). That is, the solar spectrum had greater overlap with the absorption spectrum of *D. salina* particularly for the shorter wavelengths (400–500 nm), thereby more effectively simulating the *D. salina* reaction centers for a given irradiance (Fig. 3) [13]. This may also explain the fact that the maximum photosynthetic rate (P_{max}) was reached at a lower irradiance (~230 μE m^{-2} s^{-1}) for the solar spectrum, compared to ~260 μE m^{-2} s^{-1} for the LSC spectrum. However, the magnitude of P_{max} for the two treatments did not appear to differ significantly (solar spectrum P_{max} = 166 ± 15.18 μmol O_2 L^{-1} h^{-1}; LSC medium spectrum P_{max} = 135 ± 33.92 μmol O_2 L^{-1} h^{-1}), in part due to the large standard error for the LSC medium PI parameters due to the noisier data. Decreasing O_2 production rates due to photoinhibition (the slope of which is given by β) (solar: 0.11 ± 0.03 μmol O_2 L^{-1} h^{-1}/(μE m^{-2} s^{-1}); LSC medium: 0.22 ± 0.11 μmol O_2 L^{-1} h^{-1}/(μE m^{-2} s^{-1})) was also not different between treatments (Fig. 6). Overall, these photosynthetic behavior experiments corroborate our findings from the greenhouse experiments, indicating that photosynthetic activity is similar for algae receiving light filtered through LSC medium panels compared to the solar spectrum.

The programmable 16-LED array is a useful tool that can aid in the identification of new dye combinations that divert wavelengths not useful for generation of desired byproducts to electricity generation. Future experiments will focus on fine-tuning dye type and dye concentration for simultaneously optimizing electricity production, biomass growth, and even target specific algal byproducts of commercial interest.

4. Conclusion

Microalgae and cyanobacteria grew as well or better under wavelength selective LSC panels containing the dye LR305, compared to the full solar spectrum, while harnessing green wavelengths for energy production. Chl *a* concentration was higher in some cultures but no clear effect on carotenoid to chl *a* ratios was observed for cells grown under LSC panels. Paddlewheels, fans, sensors and other electronic devices for both control and LSC greenhouse operations were powered by the PV cells on the LSC greenhouse during the algal growth trials, further demonstrating the capacity for these wavelength selective photovoltaic panels to produce enough electricity to power greenhouse operations while maintaining equivalent biomass yields as a clear, standard type greenhouse. This is the first time, to our knowledge, that algae growth has been assessed in greenhouses covered with wavelength selective photovoltaic panels. Though the energetic profile and lower operation costs for LSC greenhouses are desirable, and addressed more fully in other literature [10], potential adopters will need guarantees on quality and yield of the algal commercial crop viability, which we have demonstrated in this study.

Conflicts of interest

The authors declare no competing financial interest.

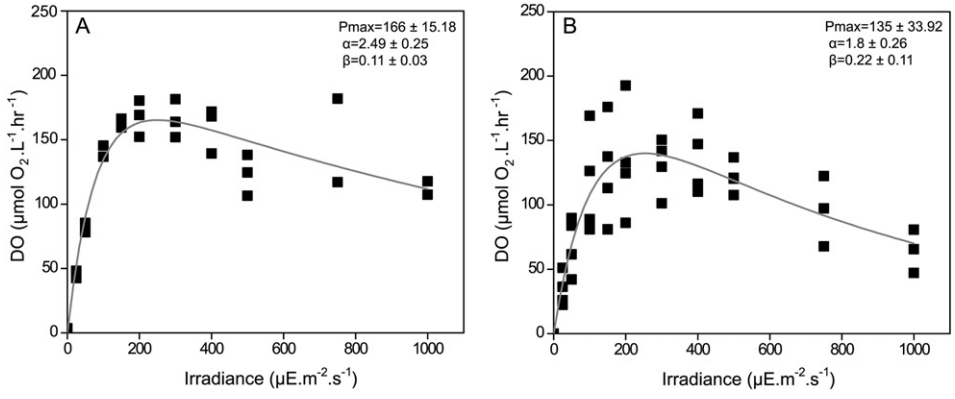

Fig. 6. Photosynthesis–irradiance curves for *D. salina* under a simulated solar spectrum (A) and the LSC medium spectrum (B). P_{max} is the maximum photosynthetic rate (μmol O_2 L^{-1} h^{-1}); α is the positive slope of the curve prior to photoinhibition (μmol O_2 L^{-1} h^{-1}/(μE m^{-2} s^{-1})), and β is the negative slope in response to photoinhibition (μmol O_2 L^{-1} h^{-1}/(μE m^{-2} s^{-1})). Values are represented as the average (N = 3 for the solar spectrum; N = 4 for the LSC medium spectrum) ± standard error.

Acknowledgments

This study was funded by the UC Discovery Grant "Low cost, high efficiency luminescent solar greenhouse" (grant # 192864) to Dr. Sue Carter in collaboration with the Algae for Exploration (AlEx) working group in the Exobiology Branch at NASA ARC. Dr. Carter received additional funding from Abengoa Solar. The authors would like to thank Glenn Alers for making available the LSC panels used in this study, Stuart Pilorz for the help with data analysis, and Craig Everroad and Thomas Murphy for their insightful comments in reviewing this manuscript.

References

[1] A. Vonshak, A. Richmond, Mass production of the blue-green alga *Spirulina*: an overview, Biomass 15 (1988) 233–247.
[2] P. Spolaore, C. Joannis-Cassan, E. Duran, A. Isambert, Commercial applications of microalgae, J. Biosci. Bioeng. 101 (2) (2006) 87–96.
[3] M.A. Zeller, R. Hunt, A. Jones, S. Sharma, Bioplastics and their thermoplastic blends from *Spirulina* and *Chlorella* microalgae, J. Appl. Polym. Sci. 130 (5) (2013) 3263–3275.
[4] L. Lardon, A. Hélias, B. Sialve, J.-P. Steyer, O. Bernard, Life-cycle assessment of biodiesel production from microalgae, Environ. Sci. Technol. 43 (17) (2009) 6475–6481.
[5] O. Jorquera, A. Kiperstok, E.A. Sales, M. Embiruçu, M.L. Ghirardi, Comparative energy life-cycle analyses of microalgal biomass production in open ponds and photobioreactors, Bioresour. Technol. 101 (2010) 1406–1413.
[6] P.K. Campbell, T. Beer, D. Batten, Life cycle assessment of biodiesel production from microalgae in ponds, Bioresour. Technol. 102 (2011) 50–56.
[7] W.H. Weber, J. Lambe, Luminescent greenhouse collector for solar radiation, Appl. Opt. 15 (10) (1976) 2299–2300.
[8] W.G.J.H.M. van Sark, K.W.J. Barnham, L.H. Slooff, A.J. Chatten, A. Büchtemann, A. Meyer, S.J. McCormack, R. Koole, D.J. Farrell, R. Bose, E.E. Bende, A.R. Burgers, T. Budel, J. Quilitz, M. Kennedy, T. Meyer, C. De Mello Donegá, A. Meijerink, D. Vanmaekelbergh, Luminescent solar concentrators — a review of recent results, Opt. Express 16 (26) (2008) 21773–21792.
[9] M.J. Currie, J.K. Mapel, T.D. Heidel, S. Goffri, M.A. Baldo, High-efficiency organic solar concentrators for photovoltaics, Science 321 (2008) 226–228.
[10] C. Corrado, S.W. Leow, M. Osborn, E. Chan, B. Balaban, S.A. Carter, Optimization of gain and energy conversion efficiency using front-facing photovoltaic cell luminescent solar concentrator design, Sol. Energy Mater. Sol. Cells 111 (2013) 74–81.
[11] K.J. McCree, The action spectrum, absorptance and quantum yield of photosynthesis in crop plants, Agric. Meteorol. 9 (1972) 191–216.
[12] E. Rabinowitch, G. Govindjee, Photosynthesis, John Willey and Sons, New York, NY, 1969. 102–123.
[13] H.L. MacIntyre, J.J. Cullen, Using cultures to investigate the physiological ecology of microalgae, in: R.A. Andersen (Ed.), Algal Culturing Techniques, Elsevier Academic Press, Burlington, MA, 2005, pp. 287–326.
[14] C.-G. Lee, B.O. Palsson, High-density algal photobioreactors using light-emitting diodes, Biotechnol. Bioeng. 44 (1994) 1161–1167.
[15] H.C.P. Matthijs, H. Balke, U.M. Van Hes, B.M.A. Kroon, L.R. Mur, R.A. Binot, Application of light-emitting diodes in bioreactors: flashing light effects and energy economy in algal culture (*Chlorella pyrenoidosa*), Biotechnol. Bioeng. 50 (1996) 98–107.
[16] J.M. Gordon, J.E.W. Polle, Ultrahigh bioproductivity from algae, Appl. Microbiol. Biotechnol. 76 (2007) 969–975.
[17] W. Fu, O. Guomundsson, G. Paglia, G. Herjolfsson, O.S. Andresson, B.O. Palsson, S. Brynjolfsson, Enhancement of carotenoid biosynthesis in the green microalga *Dunaliella salina* with light-emitting diodes and adaptive laboratory evolution, Appl. Microbiol. Biotechnol. 97 (2013) 2395–2403.
[18] T. Katsuda, A. Lababpour, K. Shimahara, S. Katoh, Astaxanthin production by *Haematococcus pluvialis* under illumination with LEDs, Enzym. Microb. Technol. 35 (2004) 81–86.
[19] P. Das, W. Lei, S.S. Aziz, J.P. Obbard, Enhanced algae growth in both phototrophic and mixotrophic culture under blue light, Bioresour. Technol. 102 (2011) 3883–3887.
[20] E. Eroglu, S. Okada, A. Melis, Hydrocarbon productivities in different *Botryococcus* strains: comparative methods in product quantification, J. Appl. Phycol. 23 (2011) 763–775.
[21] U.G. Schlosser, Sammlung von Algenkulturen, Ber. Dtsch. Bot. Ges. 95 (1982) 181–276.
[22] A.D. Steinman, G.A. Lamberti, Biomass and pigments of benthic algae, in: F.R. Hauer, G.A. Lamberti (Eds.), Methods in Stream Ecology, Academic Press, San Diego, CA, 1996, pp. 295–313.
[23] H.K. Lichtenthaler, C. Buschmann, Chlorophylls and carotenoids: measurement and characterization by UV–VIS spectroscopy, Current Protocols in Food Analytical Chemistry, 2001, pp. F4.3.1–F4.3.8. http://dx.doi.org/10.1002/0471142913.faf0403s01.
[24] N.A. Welschmeyer, Fluorometric analysis of chlorophyll *a* in the presence of chlorophyll *b* and pheopigments, Limnol. Oceanogr. 39 (1994) 1985–1992.
[25] R.K. Clayton, Photosynthesis: Physical Mechanisms and Chemical Patterns, Cambridge University Press, London, 1980. 281.
[26] T. Platt, C.L. Gallegos, W.G. Harrison, Photoinhibition of photosynthesis in natural assemblages of marine phytoplankton, J. Mar. Res. 38 (1980) 687–701.
[27] J.-J. Frenette, S. Demers, L. Legendre, J. Dodson, Lack of agreement among models for estimating photosynthetic parameters, Limnol. Oceanogr. 38 (3) (1993) 679–687.
[28] C.E. Buckley, J.A. Houghton, A study of the effects of near UV radiation on the pigmentation of the blue-green alga *Gloeocapsa alpicola*, Arch. Microbiol. 107 (1976) 93–97.
[29] H.W. Paerl, J. Tucker, P.T. Bland, Carotenoid enhancement and its role in maintaining blue-green algal (*Microcystis aeruginosa*) surface blooms, Limnol. Oceanogr. 28 (1983) 847–857.
[30] H.W. Paerl, Cyanobacterial carotenoids: their roles in maintaining optimal photosynthetic production among aquatic bloom forming genera, Oecologia 61 (2) (1984) 143–149.
[31] B.M. Smith, P.J. Morrissey, J.E. Guenther, J.A. Nemson, M.A. Harrison, J.F. Allen, A. Melis, Response of the photosynthetic apparatus in *Dunaliella salina* (green algae) to irradiance stress, Plant Physiol. 93 (1990) 1433–1440.
[32] B. Richardson, D.M. Orcutt, H.A. Schwertner, C.L. Martinez, H.E. Wickline, Effects of nitrogen limitation on the growth and composition of unicellular algae in continuous culture, Appl. Microbiol. 18 (2) (1969) 245–250.
[33] Z. Kolber, J. Zehr, P. Falkowski, Effects of growth irradiance and nitrogen limitation on photosynthetic energy conversion in photosystem II, Plant Physiol. 88 (1988) 923–929.
[34] L. Poryvkina, S. Babichenko, A. Leeben, Analysis of phytoplankton pigments by excitation spectra of fluorescence, Proceedings of EARSeL-SIG-Workshop LIDAR, Dresden/FRG, June 16–17, 2000.